SANDIA REPORT

SAND95–1649 • UC–920
Unlimited Release
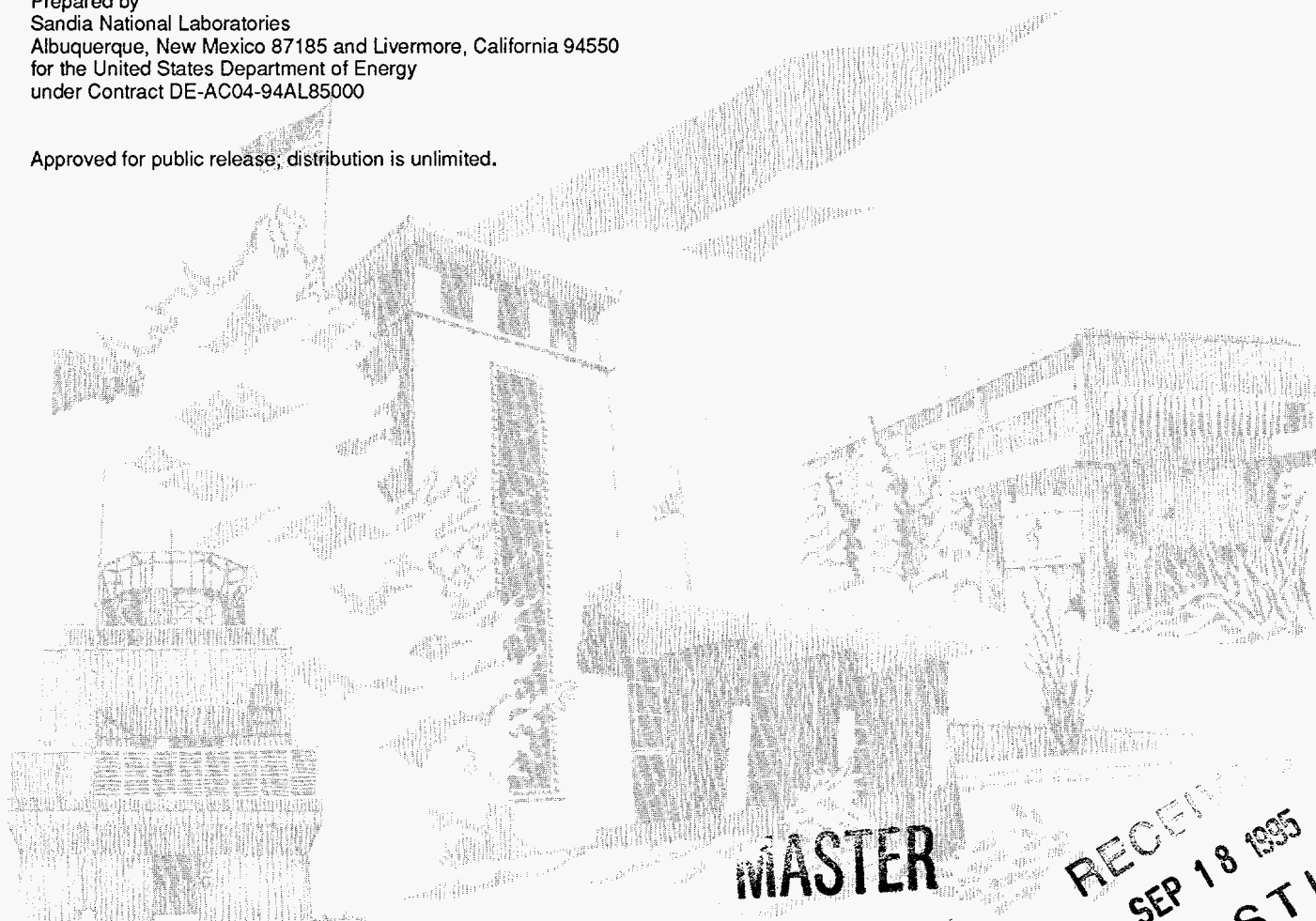Printed August 1995

Thermal Conductivity of Thermal-Battery Insulations

Ronald A. Guidotti, Marvin Moss

MASTER

SF2900Q(8-81)

DISCLAIMER

Portions of this document may be illegible in electronic image products. Images are produced from the best available original document.

Thermal Conductivity of Thermal-Battery Insulations

Ronald A. Guidotti
Battery Research Department

Marvin Moss
Patent and Licensing Center

Sandia National Laboratories
Albuquerque, NM 87175-5800

Abstract

The thermal conductivities of a variety of insulating materials used in thermal batteries were measured in atmospheres of argon and helium using several techniques. (Helium was used to simulate the hydrogen atmosphere that results when a Li(Si)/FeS$_2$ thermal battery ages.) The guarded-hot-plate method was used with the Min-K insulation because of its extremely low thermal conductivity. For comparison purposes, the thermal conductivity of the Min-K insulating board was also measured using the hot-probe method. The thermal-comparator method was used for the rigid Fiberfrax board and Fiberfrax paper. The thermal conductivity of the paper was measured under several levels of compression to simulate the conditions of the insulating wrap used on the stack in a thermal battery. The results of preliminary thermal-characterization tests with several silica aerogel materials are also presented.

Acknowledgments

Contents

Figures

Figures (continued)

Tables

Thermal Conductivity of Thermal-Battery Insulations

Introduction

Thermal batteries use a variety of thermal-insulation materials in their construction. Insulating discs are used at the ends of the stack and between end heat pellets to retard heat loss. These discs typically are alumino-silicate materials (e.g., Fiberfrax board) or a composite material such as Min-K or Microtherm. The latter consist of a molded mixture of fumed silica and titania (made by high-temperature steam hydrolysis of the metal halides) mixed with quartz fibers and are the best commercial thermal insulation available other than a vacuum insulation.

The battery stack also utilizes a flexible ceramic blanket (e.g., Fiberfrax paper) for insulating purposes. This blanket typically is wrapped tightly around the stack and held in place with glass tape. An alternative insulation for the stack is a sleeve of Min-K or Microtherm. The sleeve is used when the lifetime of the battery is to be maximized, such as for a long-life (greater than one hour) application.

For thermal-modelling purposes,[1] it is desirable to accurately know the thermal conductivity of these materials as a function of temperature. Only some of the necessary data for an air environment are available from the manufacturers. During storage of a $Li(Si)/FeS_2$ thermal battery, however, residual moisture reacts with the Li(Si) anode to generate an atmosphere of hydrogen. The thermal conductivities of the various insulating materials under a hydrogen atmosphere are generally not available. In addition, the effects of compression on the thermal conductivity of the ceramic blanket are not known. This is important for thermal-battery applications, since the blanket is tightly wrapped around the stack and is compressed during assembly.

The purpose of the study documented here was to measure the thermal conductivity as a function of temperature and atmosphere of both the rigid and flexible insulations used in thermal batteries. In addition, the effects of compression upon the thermal properties of the flexible ceramic blanket were examined. Preliminary thermal-characterization experiments were also carried out with several silica aerogel materials.

Experimental Procedures

Materials

The commercial insulating materials that were examined in this work are listed in Table 1. Before the measurement of thermal conductivity, the Fiberfrax board and paper were heated at 600°C for four hours in a dry-room environment. In the case of the Min-K TE1400 board, the baking time was increased to nine hours.

The aerogels were prepared by ammonia hydrolysis of silicon alkoxides in aqueous methanol or ethanol solutions.[2,3] In some samples, fumed TiO_2 or carbon black was added to test as thermal opacifiers. The mixture was then allowed to age and form a silica polymer network. Final gelation usually occurred within 30 minutes. After aging at 50°C for several days, the solvents and water were removed from the gels by supercritical extraction with carbon dioxide at 7.584 MPa (1100 psig) at 38°C.

1

TABLE 1. Commercial Insulation Materials Examined for the Thermal-Conductivity Study

Insulation	Nominal Density, g/cc	Nominal Thickness, mm*	Manufacturer
Fiberfrax T-30LR laminate (51.7% Al_2O_3/47.6% SiO_2)	0.80	3.0	Carborundum Co., Niagara Falls, NY
Fiberfrax 970-H paper (51.7% Al_2O_3/47.6% SiO_2)	0.16	1.5	Carborundum Co., Niagara Falls, NY
Min-K TE1400 board (83.9% SiO_2/15.8% TiO_2)	0.32	8.0	Schuller Specialty Insulations, Denver, CO

* Uncompressed state.

Measurement Techniques

Thermal Comparator. The thermal-comparator technique was used for the bulk of the thermal-conductivity measurements.[4] This basically consists of measuring the heat flow across a sample subjected to a controlled thermal gradient.[5,6] A Dynatech Model TCFCM-N20 (Cambridge, MA) was used to perform the measurements. The comparator technique has an accuracy of approximately 7%.

Guarded Hot Plate. A second technique for measuring thermal conductivity was the guarded-hot-plate method.[7] This method was used for the Min-K board, because it is more accurate for materials of low thermal conductivity (<0.1 W/m-K). This method uses a guard heater to maintain the sample under adiabatic conditions. A Dynatech Model TCFGM-N18 (Cambridge, MA) was used for these measurements.

Before testing the insulations in atmospheres other than air, the insulations were baked out under a high vacuum in the test chamber to remove adsorbed gases. The test chamber was backfilled with the test gas (either argon or helium) to start the test.

Hot Probe. A third technique used to measure thermal conductivity was the hot-probe method.[8,9] This technique involves insertion of a heated probe into the test material and measuring the radial heat flux over the desired temperature range. The hot-probe technique was suitable for use with only the Min-K board and had an estimated accuracy of about 10%. The hot probe was custom fabricated; a schematic representation of the hot probe is shown in Figure 1. Only a limited number of experiments was performed using this technique.

CONSTANTAN PROBE
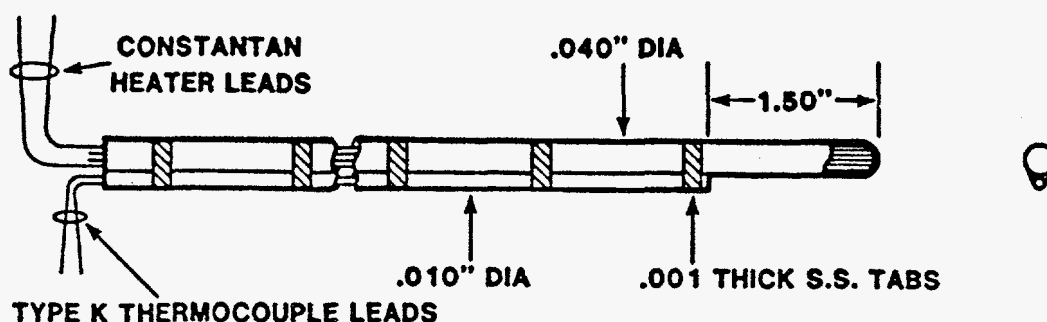
FIGURE 1. Construction Detail of High-Temperature Constantan Prober

Heated-Block and Heated-Platen Set-ups.
Several other experimental setups were used to obtain a relative measure of the thermal-transfer properties of the various insulations. The setup illustrated in Figure 2 consists of an aluminum block heated with cartridge heaters and surrounded by the insulation being tested. This setup was designed for testing insulation in the form of wrapped blankets or sleeves. The temperature drop across the insulation was measured with two thermocouples, one on each side of the test material. The temperature range of interest in the study was 300°C–500°C, which brackets the typical operating temperature range of a thermal battery. These tests were conducted in ambient air; temperatures were measured in both the heating and cooling modes to ensure that accurate steady-state conditions were attained.

The setup involving the heated platen is shown in Figure 3. This setup consists of a heated stainless-steel platen in contact with one side of the sample sandwiched between two 0.5-mm-thick copper discs. The opposite side of the sample was in contact with a 25-mm-thick block of Min-K TE1400 insulation. The samples used were 6-mm-thick discs measuring 22.2 cm in diameter. A temperature range of 400°C–550°C was used for these tests; the temperature differential between the heated platen and the bottom of the sample was monitored in both the heating and cooling modes. These tests were conducted in a glovebox under high-purity argon.

Compression. The effect of compression of the ceramic paper on the thermal conductivity was determined by applying different loads to the paper. The amount of compression was varied from about 47% to 65% of the original 0.6-cm total thickness, which was made up of four thicknesses of paper.

Atmosphere. The effect of argon and helium atmospheres on the thermal conductivity of the paper was examined. Helium was used instead of hydrogen because of safety concerns and is the gas with the closest thermal conduc-tivity to hydrogen. The thermal conductivities of the various gases are listed in Table 2 for a temperature of 60°C.

The manner in which Min-K is manufactured results in a laminar structure. Consequently, it would be expected to exhibit non-isotropic thermal properties. To investigate this possibility, the thermal conductivity was measured both perpendicular and parallel to the lamination direction.

3

Heat-Transfer Setup

Control thermocouple

Measurement TC #1

Min-K Pad

Insulating Sleeve Under Test

Cartridge Heaters

Al Block

Min-K Pad

Measurement TC #2

FIGURE 2. Experimental Setup for Heated-Block Fixture for Heat-Transfer Tests

Test Setup for Evaluation of Aerogel Discs

Heated Platen

Platen Thermocouple

Cu

Sample

Cu

Sample Thermocouple

Insulating Disc
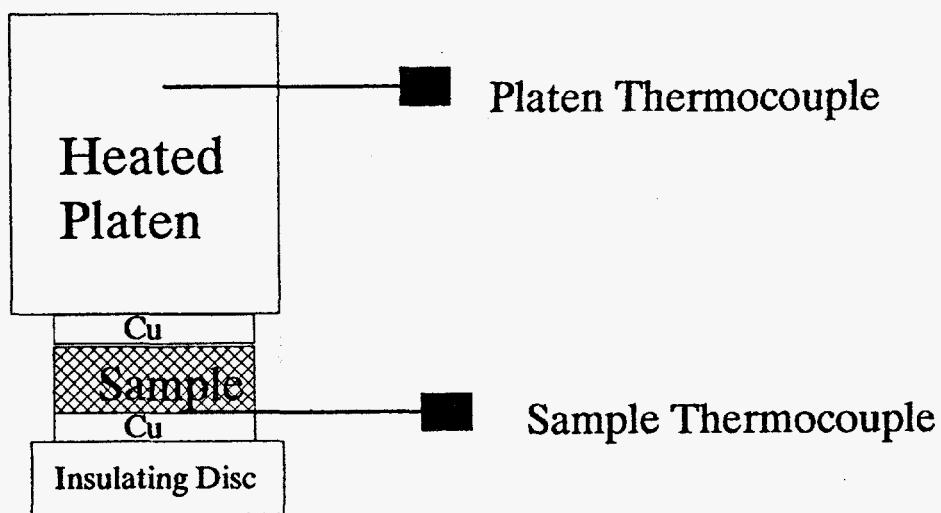
FIGURE 3. Experimental Setup for Heated-Platen Fixture for Heat-Transfer Tests

4

TABLE 2. Thermal Conductivities of Various Gases at 60°C[10]

Gas	Thermal Conductivity, mW/m-K
Hydrogen	202.5
Helium	159.8
Air	28.4
Argon	19.6
Krypton	6.0

Results

Fiberfrax Board

The thermal conductivity of the Fiberfrax board is shown in Figure 4 as a function of temperature for atmospheres of argon and helium. The corresponding manufacturer's data for an atmosphere of air are shown for comparison.
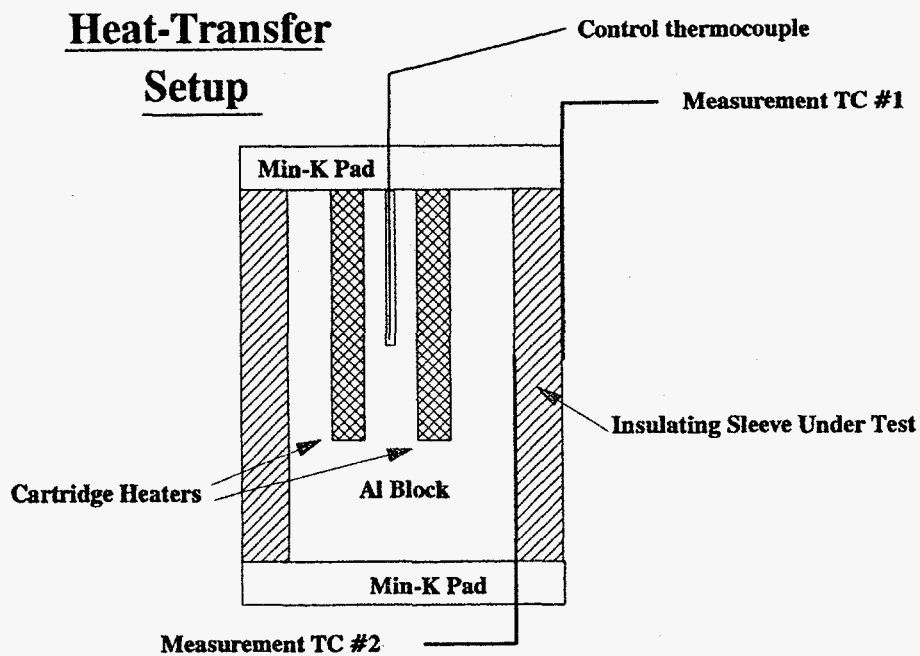
The effects of the thermal conductivity of the gas on the thermal conductivity of the board were significant. The use of helium in place of argon increased the thermal conductivity of the board by a factor of two over the temperature range measured. The manufacturer's reported thermal conductivity of the board in air was less than the thermal conductivity that we measured in argon. Since the thermal conductivity of air is higher than that of argon (Table 2), one would expect that the thermal conductivities of the board measured in argon would be lower than those in air. This apparent anomaly may be due to the sample history. Our sample was baked at a high temperature (600°C), which could have changed its thermal properties. The corresponding history of the manufacturer's sample is not known.

The measured thermal conductivities would indicate that the porosity of the Fiberfrax board is sufficient to allow rapid conduction through the gas phase; i.e., the mean diffusion path of the gas molecules is much smaller than the median pore size of the Fiberfrax board.

Fiberfrax Paper

The thermal conductivity of four layers of Fiberfrax paper is shown as a function of temperature for atmospheres of argon and helium in Figures 5 and 6, respectively, for compressions of 47% and 65% (relative to an uncompressed thickness of 0.60 cm). The manufacturer's thermal-conductivity data for the uncompressed material in air are also included for comparison in Figure 5.

The effect of compression was more pronounced for the argon atmosphere, where a 21–33% increase in conductivity of the paper was observed when the degree of compression was increased from 47% to 65%. The change in thermal conductivity was only 7–12% for the same compression in a helium atmosphere

The relative increase of thermal conduc-tivity in going from an argon atmosphere to one of helium was much more pronounced for the Fiberfrax paper than that noted for the Fiberfrax board (Figure 4). This is a result of the more ready access to the larger pores of the paper insulation, compared with those of the board.

The manufacturer's values for the thermal conductivity of the uncompressed paper in air were close to the values of the compressed paper measured in an atmosphere of argon (Figure 5).
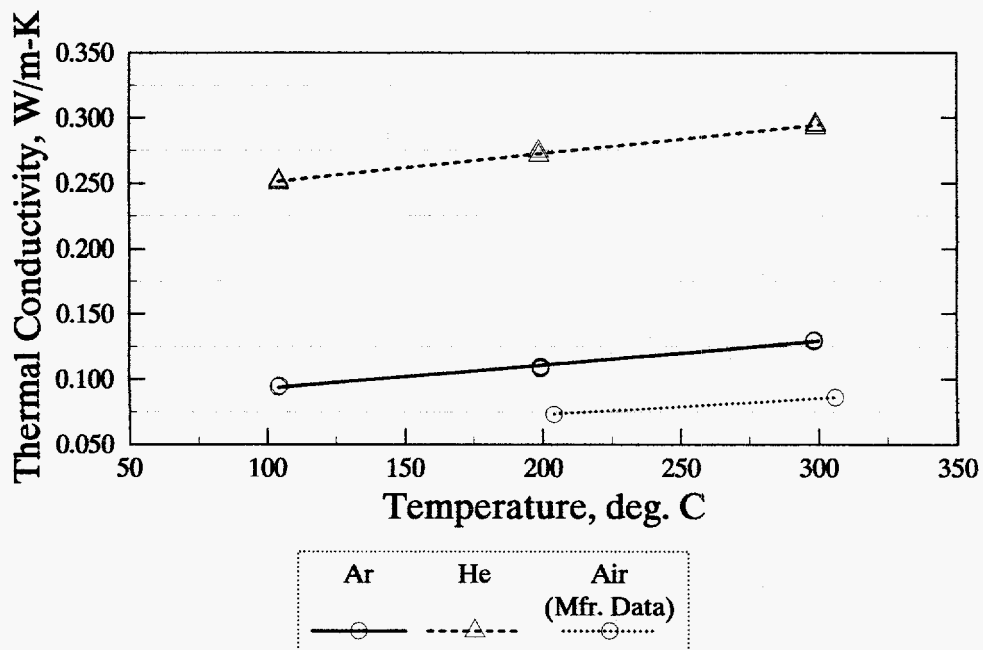
FIGURE 4. Thermal Conductivity of Fiberfrax Board as a Function of Atmosphere and Temperature
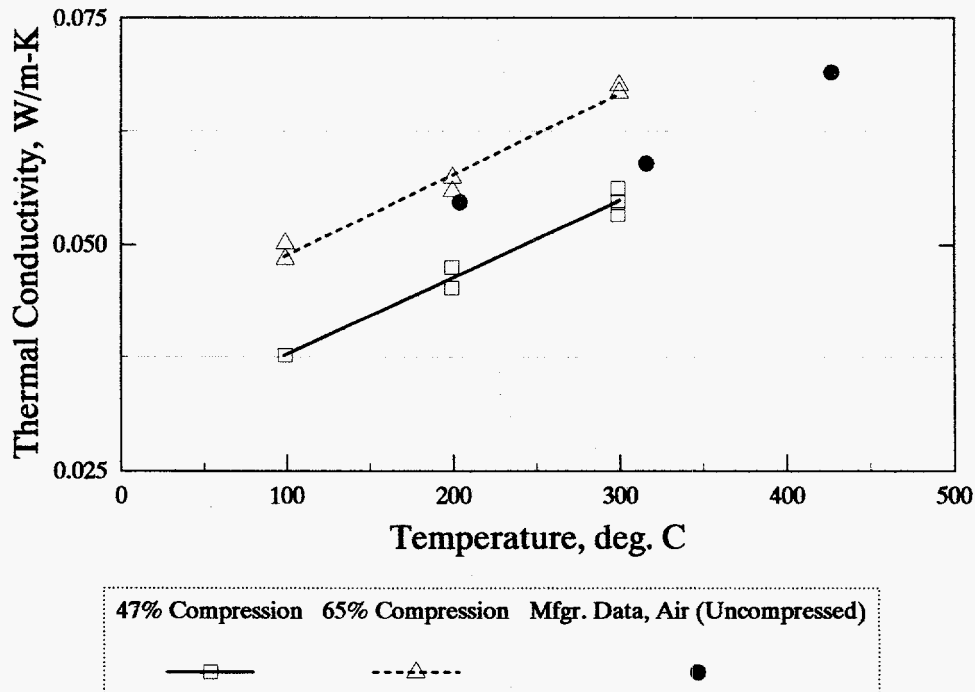
FIGURE 5. Thermal Conductivity of Fiberfrax Blanket in Argon as a Function of Compression and Temperature
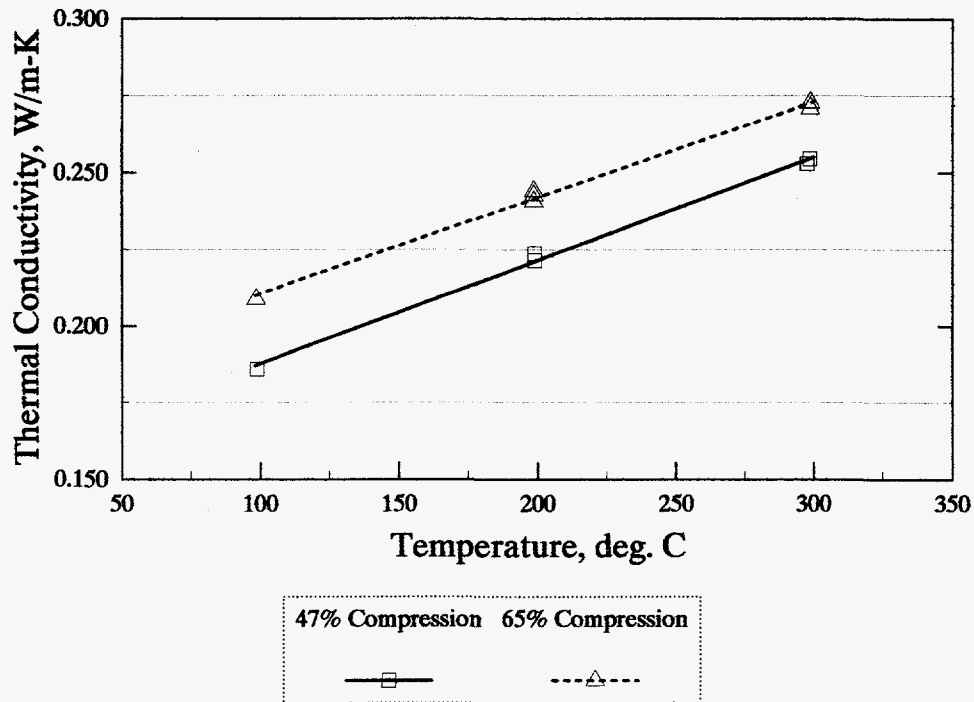
FIGURE 6. Thermal Conductivity of Fiberfrax Blanket in Helium as a Function of Compression and Temperature

Min-K TE1400 Board

The thermal conductivity as a function of temperature is shown in Figure 7 for the Min-K TE1400 composite board for atmospheres of argon and helium. Data are reported for thermal conductivity perpendicular to the lamination direction (as would normally be measured) as well as parallel to the laminations. The data were obtained using the guarded-hot-plate technique, since the comparator method is not suitable for materials with thermal conductivities of <0.1 W/m-K.

The thermal conductivity of Min-K in helium was much greater than that in argon. The effect was more pronounced in the parallel direction than in the perpendicular direction. The temperature dependence was also more pro-nounced for the parallel direction.

The thermal conductivities for Min-K TE1400, along with manufacturer's data, are replotted in Figure 8 for a wider temperature window. Similar data from Skrabek et al. and data for air are included for comparison.[11] The data in argon are comparable to those in air. Our data in argon agree well with those in air reported by Skrabek et al. when extrapolated. Skrabek's thermal-conductivity data in helium, however, are much higher than ours.

The thermal conductivity of Min-K TE1400 that we measured at ambient temperature (28°C) in air by the hot-probe technique is compared in Table 3 to similar data (extrapolated from higher temperatures) reported by the manufacturer and Skrabek et al. The agreement is very good, considering possible extrapolation errors and that this is intrinsically a difficult material to measure. Note that the increased loss in heat (higher thermal conductivity) in the parallel direction corroborates the findings made with the guarded hot plate (Figure 7).

7
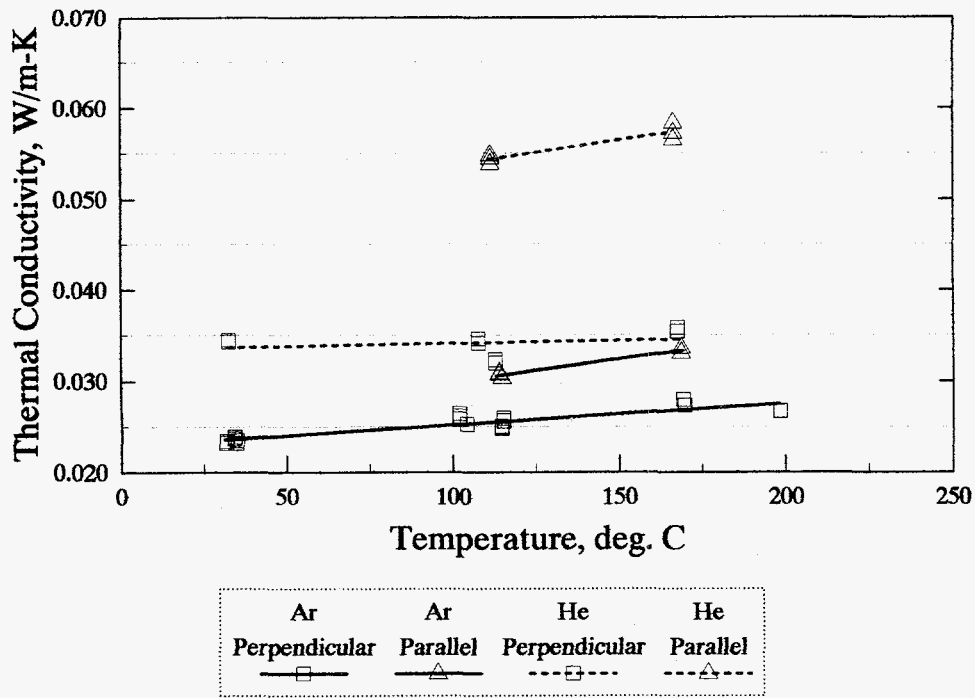
FIGURE 7. Thermal Conductivity of Min-K TE1400 Board in Helium and Argon as a Function of Temperature and Orientation

Perpendicular to laminations.
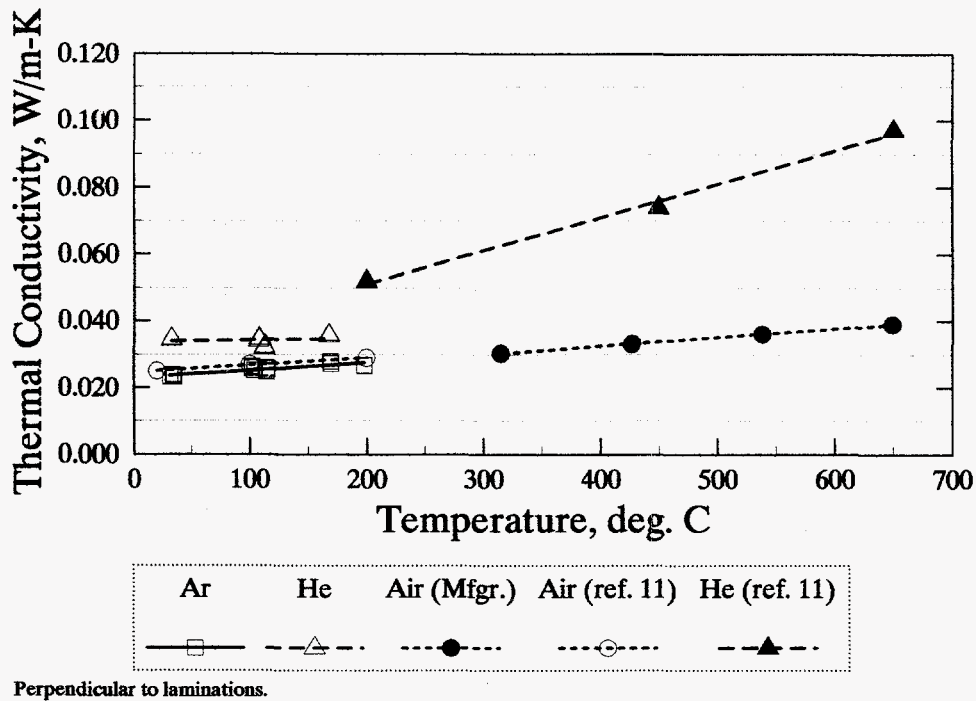
FIGURE 8. Thermal Conductivity of Min-K TE1400 Board as a Function of Atmosphere and Temperature

8

TABLE 3. Comparison of Thermal Conductivity of Min-K TE1400 Measured in Air by Hot Probe Technique With That Reported by Other Sources

Source of Data	Lamination Direction	Thermal Conductivity at 28°C, mW/m-K
Sandia	Perpendicular	23.5
Sandia	Parallel	26.5
Manufacturer	Perpendicular	22.7 (extrapolated)
Ref. 11	Perpendicular	25.3 (extrapolated)

The insulation effectiveness of the Min-K board can be improved with gases with lower thermal conductivities or with vacuum. Data from Skrabek et al. are plotted in Figure 9 for atmospheres of xenon, helium, and air, as well as for a vacuum. The relative differences in thermal conductivity of the Min-K board in xenon and under vacuum are quite small.

Insulation Comparisons

Argon. The thermal conductivities of the various thermal-battery insulations in an argon atmosphere are compared in Figure 10. The thermal conductivities for Min-K are shown only for the direction perpendicular to the laminations. The poorest thermal insulator was the Fiberfrax board, and the best was the Min-K TE1400. The relative trends are what one would expect for these types of materials.

Helium. Comparable thermal conduc-tivities in a helium atmosphere are presented in Figure 11. The Fiberfrax family of insulations was more closely clustered together in a helium atmosphere than was observed in an atmosphere of argon. This was probably a result of more ready access to the pores of these materials by helium than by argon.

Ancillary Tests. A number of silica aerogels were selected for evaluation because of the potential that they have as insulating material.[2,3] Typical aerogels have a density of 5–10% of theoretical; i.e., 90–95% of the material is void space. Thermal conductivities of as low as 13.1 mW/m-K have been reported for a temperature range of −20°C to +50°C.[12] This is less than half of that for Min-K. There are several disadvantages with silica aerogels, however. One is their fragility when unsupported, and the other is their transparency to infrared radiation in the range of 3–7 μm.[12,13]

The results of complementary tests with the heated aluminum block (Figure 2) are summarized in Figure 12 for the materials listed in Table 4. Two sleeves of silica aerogel were placed on top of each other for this test, because it was not possible to fabricate a single piece with the desired height of 10 cm. The thermal responses of the Min-K TE1400 and the Microtherm sleeves were similar, with a much lower temperature differential than for the sleeve of silica aerogel. This confirms the high loss of infrared (IR) energy through the silica aerogel because of the IR-transparency problems previously mentioned. As expected, the greatest temperature differential was observed with the single wrap of compressed Fiberfrax paper.
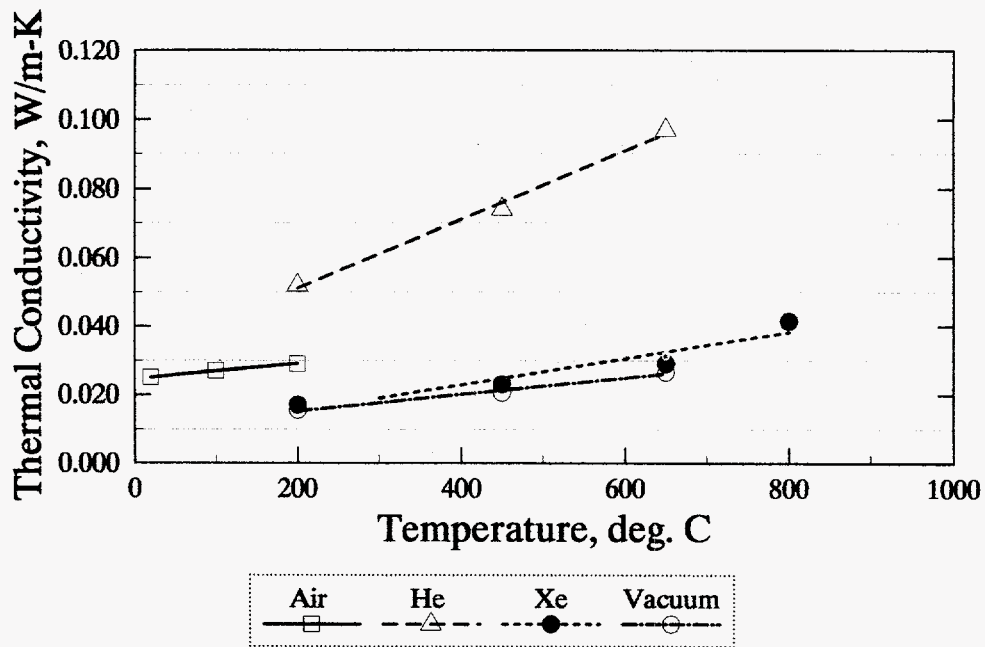
FIGURE 9. Thermal Conductivity of Min-K TE1400 Board Up to 1,000°C for Various Atmosphere and Vacuum

FIGURE 10. Thermal Conductivities of Various Insulations in Argon as a Function of Temperature

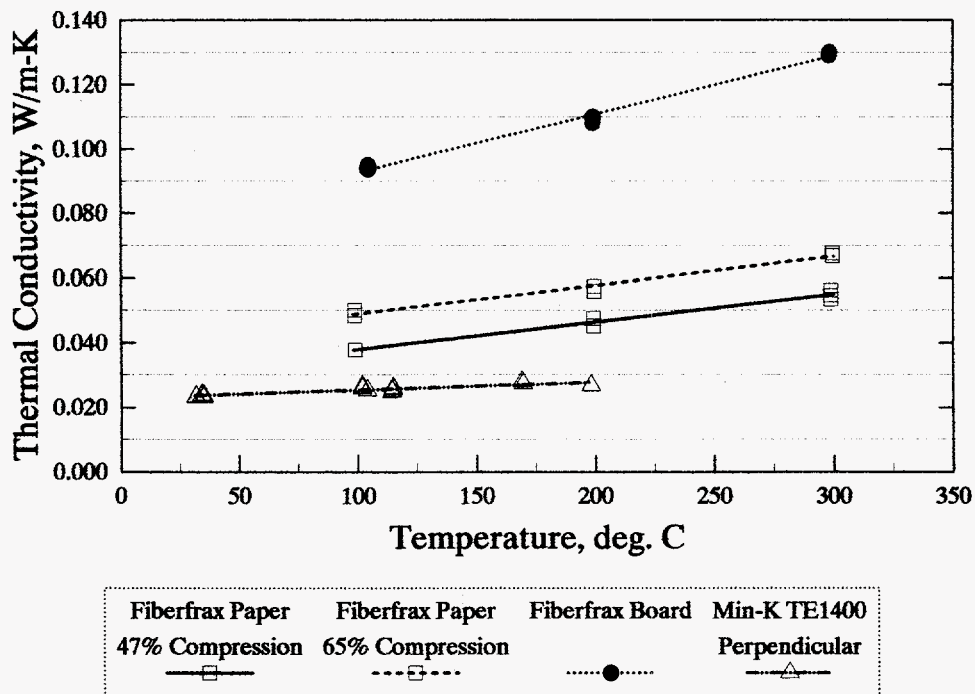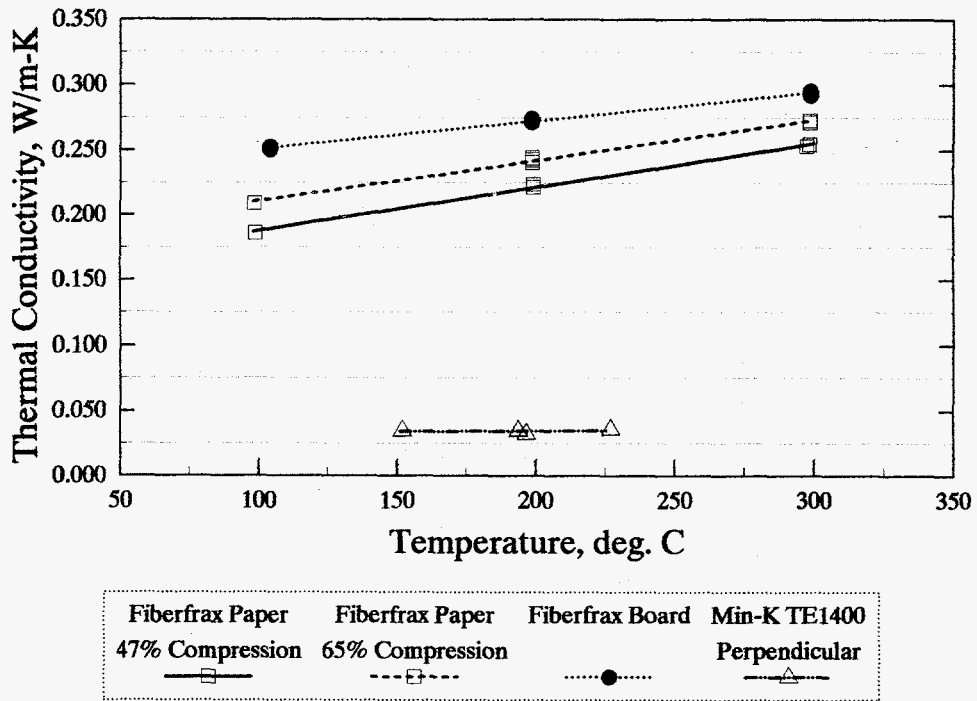**FIGURE 11. Thermal Conductivities of Various Insulations in Helium as a Function of Temperature**
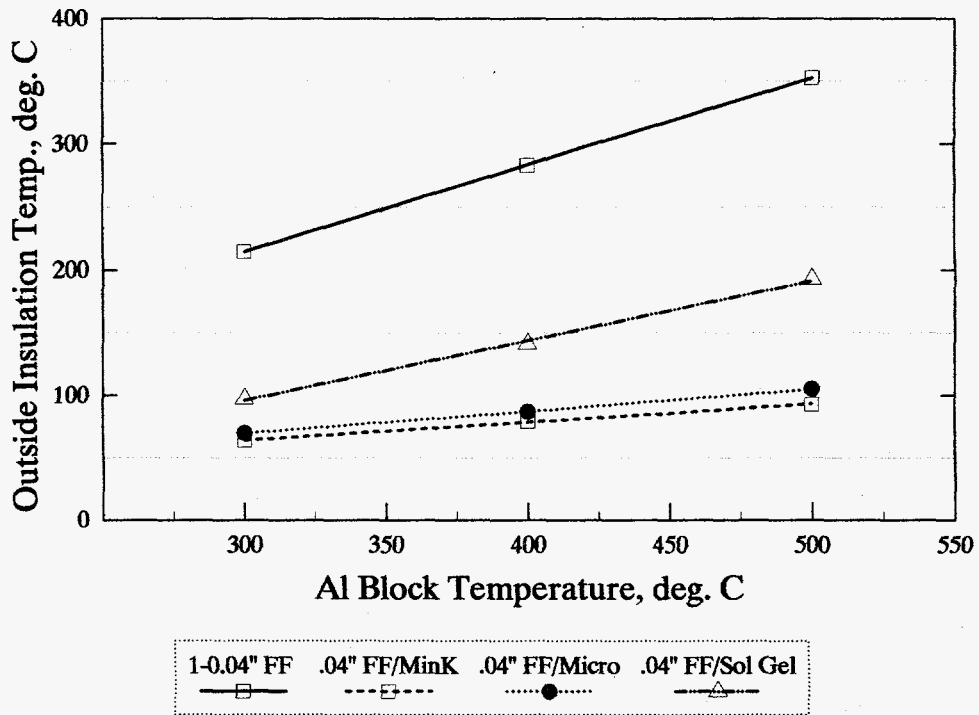
FIGURE 12. External Temperature (Center) of Insulation Sleeves as a Function of Block Temperature During Heated-Block Tests

TABLE 4. Materials Tested With the Heated-Aluminum-Block Setup of Figure 2*

Configuration	Material
1	One wrap of 1-mm-thick Fiberfrax paper (compressed)
2	One wrap of 1-mm-thick Fiberfrax paper (compressed), covered with an 8-mm-thick sleeve of Min-K TE1400
3	One wrap of 1-mm-thick Fiberfrax paper (compressed), covered with an 8-mm-thick sleeve of Microtherm
4	One wrap of 1-mm-thick Fiberfrax paper (compressed), covered with a 8-mm-thick sleeve of SiO_2 aerogel

*Insulation length was 10 cm.

The effect of the Fiberfrax thickness in the first configuration of Table 4 was examined using a double wrap of 1-mm-thick paper and a single wrap of 2-mm-thick paper. The results of these tests are summarized in Figure 13. The use of two wraps of blanket was not as effective as a single wrap of the same thickness.

The results of the heated-platen tests are summarized in Figure 14 for the various experimental silica aerogels listed in Table 5. A block of Min-K TE1400 was included for comparison purposes. The use of TiO_2 as a thermal opacifier was ineffective. Carbon black, however, was successful in reducing heat losses. At the higher loading, the carbon-black-filled aerogel was a better insulator than the Min-K.

Discussion

The temperature coefficients of the thermal conductivities of the various materials are summarized in Table 6, along with the regression coefficients for a linear least-squares fit.

In an argon atmosphere, the largest temperature coefficient for thermal conductivity was exhibited by the Fiberfrax board, followed by the paper and the Min-K board. The effect of temperature was not noticeably different for the two levels of compression examined in this study. The higher coefficient for the Min-K board in the direction parallel to the laminations accentuates the higher thermal conductivity in this direction; i.e., the higher heat losses (relative to the direction perpendicular to the laminations) are enhanced at higher temperatures.

In a helium atmosphere, the trends in the coefficients of the thermal conductivity were different from those observed in argon. The much higher thermal conductivity of the helium and smaller size of the molecule results in higher rates of heat transfer as the temperature increased for the Fiberfrax board and paper. This effect is not pronounced in the case of the Min-K board (relative to argon) because of the very small pores and more restricted access to the interior of this material. The data for the perpendicular direction contained too much scatter to make interpretation of the temperature dependence meaningful.
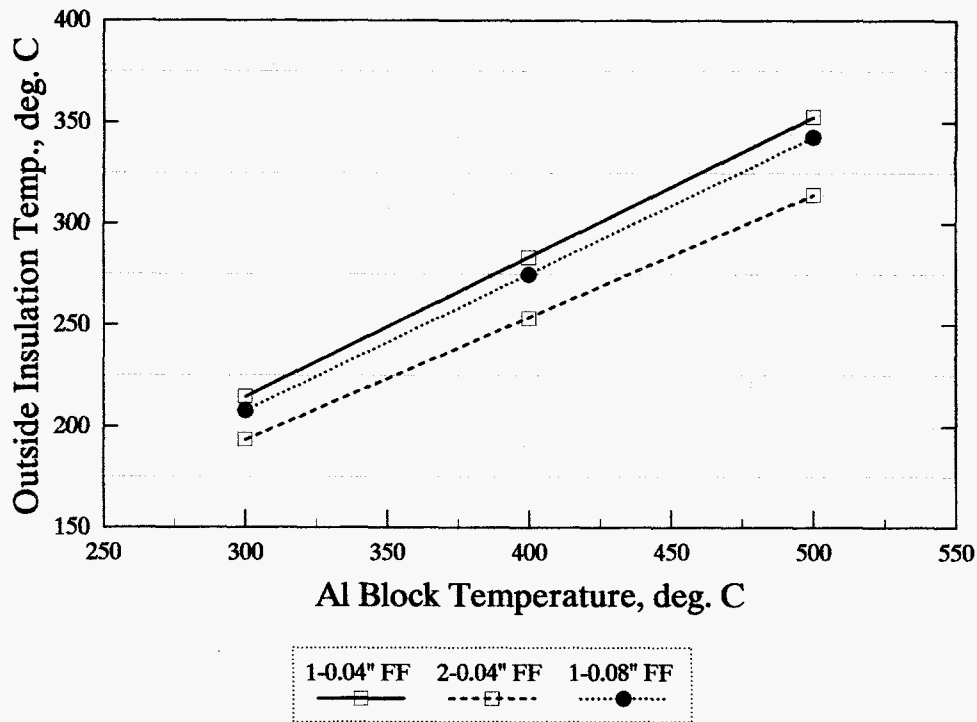
FIGURE 13. External Temperature (Center) of Fiberfrax Paper as a Function of Block Temperature for Various Thicknesses During Heated-Block Tests
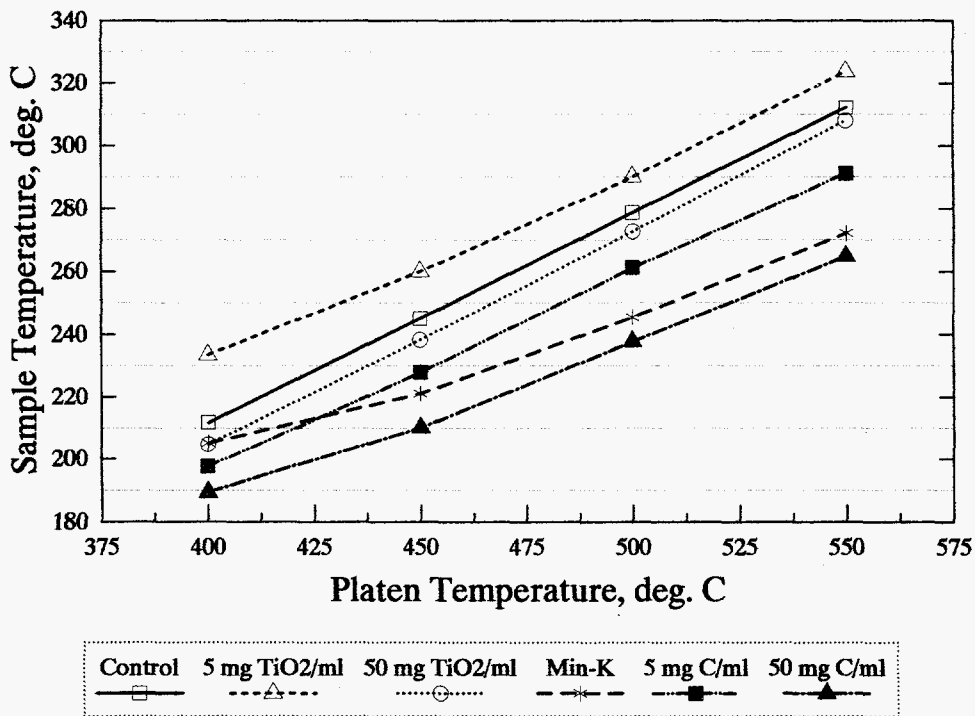
FIGURE 14. Temperature of Silica Aerogel Discs as a Function of Platen Temperature for Different Levels of Several Additives

TABLE 5. Silica Aerogel Materials Tested With the Heated Platen Setup of Figure 3*

Thermal Opacifier	Amount, mg/mL gel
None (control)	0
TiO_2	5
TiO_2	50
Carbon black	5
Carbon black	50
Min-K TE1400 control	Not applicable

*Samples were 22.2 mm in diameter and 6 mm thick.

Table 6. Temperature Coefficients for the Thermal Conductivities of Various Thermal-Battery Insulations

Material	Atmosphere	Temperature Coefficient	Regression Coefficient
Fiberfrax T-30LR laminate	Ar	18.0×10^{-5}	0.9918
Fiberfrax 970-H paper,			
47% compression	Ar	8.53×10^{-5}	0.9724
65% compression	Ar	8.92×10^{-5}	0.9808
Min-K TE1400, perpendic.	Ar	2.31×10^{-5}	0.8100
Min-K TE1400, parallel	Ar	4.85×10^{-5}	0.9668
Fiberfrax T-30LR laminate	He	21.9×10^{-5}	0.9941
Fiberfrax 970-H paper,			
47% compression	He	33.7×10^{-5}	0.9966
65% compression	He	31.2×10^{-5}	0.9954
Min-K TE1400, perpendic.	He	0.61×10^{-5}	0.0537
Min-K TE1400, parallel	He	5.45×10^{-5}	0.8624

Thermal-Battery Design Implications

The data generated in this report will prove to be very useful for incorporation into the thermal model for predicting the temperature profile of a thermal battery during discharge. The data for the thermal conductivity of compressed Fiberfrax paper should be more accurate than previous assumptions made concerning the effect of compression on thermal conductivity.

Min-K Board. The increased heat loss with the Min-K board in the direction parallel to the laminations has an immediate consequence for the design engineer. Currently, the Min-K sleeve for the thermal-battery stack is made by cutting a plug out of the block perpendicular to the

direction of lamination. This material is then machined into a sleeve. In this configuration, the radial loss of heat will be in the direction of the laminations, i.e., in the direction where the thermal conductivity is highest. It is highly unlikely that the sleeve can be machined so that the radial heat loss is in the direction perpendicular to the direction of lamination. Attempts to core a sleeve parallel to the lamination direction would result in shredding and delamination of this material. When used as end insulation, however, the heat losses will be in the direction that is perpendicular to the laminations, which is the preferred orientation.

One possible way of mitigating radial heat losses is to have the manufacturer custom mold the Min-K sleeve so that the bulk of the laminations is perpendicular to the battery stack. This would have the additional advantage that no machining would be necessary. The machining process is relatively expensive and has a yield rate for finished parts that is lower than desired.

Overgas Composition Effects. The composition of the overgases that are present in a thermal battery will affect the heat losses during discharge. Normally, thermal batteries are sealed in a dry room where the relative humidity is <3%. During storage, however, residual moisture that remains in the insulations and separator and cathode pellets slowly desorbs and reacts with the Li(Si) anode to form Li_2O and hydrogen. The oxygen that is originally present also reacts with the Li(Si). After several months, the atmosphere in the battery is composed primarily of hydrogen, nitrogen, and some argon (from the welding process). Depending on the time that the battery has been stored, the final atmosphere can vary from oxidizing to reducing.

When thermal batteries are designed and prototyped, they are usually tested shortly after construction. Consequently, the atmosphere in the battery at the time of discharge under these conditions is predominantly dry-room air.

However, when an aged battery (i.e., one more than several months old) is discharged, the atmosphere will be primarily hydrogen, which will affect the heat-transfer properties. The data generated in this study indicate that the insulation heat losses in a helium atmosphere are substantially greater than those in argon. (These two gases closely approximate the hydrogen atmosphere generated in an aged battery and the air initially present in the thermal battery.) These losses plus conduction heat losses from the stack through the overgas to the case will tend to shorten the life of the battery. This will be offset somewhat by the reduced pressure that exists once the residual oxygen and part of the nitrogen are gettered by the hot Li(Si) anode after activation.

This will generally not be a problem for a relatively short-lived battery (*e.g.*, <20 minutes). This could cause a reduction in performance, however, for batteries that are designed to run for two hours or more. Thus, the battery design engineer should verify that the heat balance is appropriate under such conditions. This can be done by aging the battery under conditions that will result in the depletion of all internal oxygen and moisture, with the concurrent generation of hydrogen overgas. This aging can be readily accomplished by heating the battery at 130°C for approximately one month.

One technique for improving the activated life of a long-life thermal battery is to reduce the heat losses that occur in the insulation and in the conduction in the overgases to the case from the stack during discharge. The accumulation of hydrogen in the battery as it ages can be offset to some degree by reducing the thermal conductivity of the overgases. One possibility is to evacuate and seal the battery under vacuum after construction. The other method involves using a backfill gas with a much lower conductivity than the normal dry-room air.

From a production standpoint, sealing a battery under vacuum, while feasible, would be a production nightmare from a quality-control perspective. It would be very difficult to leak check a system and assure a storage lifetime of >25 years, as is customarily and routinely done now. The improvement that would be realized would not be worth the expense and effort involved.

In comparison, backfilling a battery with a gas such as xenon or krypton could be accomplished much more readily. The downside to this approach, however, is the high cost of krypton and xenon. Kryton is three to four times as expensive as argon, and xenon is more expensive than krypton. Thus, there would have to be a driving need to justify the expense and additional labor involved.

Aerogel Insulation

The data generated in this work for the carbon-black-filled silica aerogel indicate that this material is very promising for possible use as insulation in thermal batteries, once its liabilities have been addressed. It should be possible to cast the aerogel directly into the battery case as a single piece. This would provide support for the aerogel and eliminate gaps that would otherwise occur with the use of several pieces of insulation, i.e., a sleeve with discs on each end.

The supported aerogel would still be susceptible to crushing or disintegration in a severe environment, such as high-*g* shock and vibration. This could be mitigated through incorporation of strengthening fibers. A tradeoff would be necessary, however, since the addition of fibers would undoubtedly increase the thermal conductivity and heat losses; i.e., the strength would be increased but at the expense of poorer thermal properties.

The ideal content of carbon black was not determined in this work. Additional work in this

area would be necessary to optimize the system, including the tradeoffs with strengthening fibers. An additional complication is that the carbon-filled aerogel would be electrically conducting, so that care would have to be taken to prevent it from contacting the battery stack to avoid intercell shorting currents. This could be accomplished by applying a thin wrap of mica or other high-temperature insulating materials such as a glass-tape or Fiberfrax wrap.

Conclusions

The thermal conductivity of the Fiberfrax paper is greatly influenced by its degree of compression. In an argon atmosphere, the thermal conductivity increases by 25–33% when the compression is increased from 47% to 65%. The thermal conductivity of all the insulations studied is much higher in helium than in argon. The thermal conductivity of the Fiberfrax board increases by a factor of 2.4, while that of the Fiberfrax paper increases by a factor of more than four. The increase for Min-K TE1400 was <1.5 because of the more restricted access to the very small pores in this material. The thermal conductivity of the Min-K depends upon the orientation of the material. In argon, the thermal conductivity parallel to the laminations is almost 30% greater than that in the perpendicular direction. This difference in helium increases by up to 60%. The temperature coefficient of thermal conductivity in argon is greatest for the Fiberfrax board, followed by the Fiberfrax paper and the Min-K board. In a helium atmosphere, the temperature coefficients of the Fiberfrax board and paper are similar and much greater than that for the Min-K board.

Silica aerogels containing carbon-black filler are promising materials for potential replacement of the Min-K TE1400 now used for long-life thermal batteries. The carbon is necessary to prevent radiation in the infrared region of 3–7 μm; fumed TiO_2 was not effective for this purpose. The fragility of these materials needs to

be addressed, however, to enable them to survive in the robust environment of a typical thermal battery. This can possibly be accomplished by the incorporation of strengthening fibers into the gel, but at the expense of the thermal properties.

Since helium has a thermal conductivity similar to that of hydrogen, there are implications for the performance of Li(Si)/FeS$_2$ thermal batteries that are more than several months old. Under these conditions, there is a significant hydrogen overgas present as a result of the reaction of the Li(Si) anodes with the adsorbed moisture that is present in the various components. The lower thermal conductivities of the thermal insulations in this environment could lead to shortening of the battery life. There is the possibility of additional heat loss from the stack to the case in the presence of hydrogen because hydrogen has a much higher thermal conductivity than air. These factors need to be considered by the thermal-battery design engineer for battery applications where thermal management is critical.

Intentionally Left Blank

References

[1]D. Bernardi, E. Pawlikowsk, and J. Newman, *J. Electrochem. Soc.,* 132 (1), 5 (1985).

[2]A. J. Hunt, C.A. Jantzen, and W. Cao, *Insulation Materials: Testing and Applications,* vol. 2, ASTM STP 1116, R. S. Graves and D. C. Wysocki, eds., American Society for Testing and Materials, Philadelphia, 1991.

[3]A. J. Hunt and M. Martin, *Proc. Intern. Symp. on Aerogels,* Sept. 30–Oct. 2, 1991, Würzburg, Germany.

[4]M. Moss, J. A. Kiski, and G. M Haseman, "Measurment of Thermal Conductivity by the Comparative Method," SAND82-0109 (March 1982)

[5]Standard ASTM C518-76, Standard Test Method for Steady-State Thermal Transmission Properties by Means of the Heat Flow Meter.

[6]J. F. Howard, K. G. Coumou, and R. P. Type, *J. Cellular Plastics,* 9, 226 (1973).

[7]Standard ASTM C177-76, Standard Test Method for Steady-State Thermal Transmission Properties by Means of the Guarded Hot Plate.

[8]W. D. Drotning, and T. V. Tormey, "Thermal Conductivity Probe Measurement System," SAND83-2057 (March 1984).

[9]H. Hayashi, M. Fukui, and T. Nishikawa, *Yogyo Gakkaishi,* 89 (8), 403 (1981).

[10]J. D. Dean, *Lang's Handbook of Chemisty,* 4th ed., p. 5.142 , McGraw-Hill, New York (1992).

[11]E. A. Skrabek, R. P. Tye, and A. O. Desjarlais, *Rev. Int. Hautes Tempér. Réfract., Fr.,* 16, 361 (1979).

[12]O. Nilsson, Å. Fransson, and O. Sandberg, *Proc. of the First Inter. Symp. on Aerogels,* Sept. 23–25, 1985, Würzburg, Germany, J. Fricke, ed., p. 121–136, Springer-Verlag, New York (1986).

[13]D, Büttner, E. Hüttner, and J. Fricke, *Ibid.,* pp. 116–120.

DISTRIBUTION:

2	Wright Laboratory
	Aero Propulsion and Power Directoratee
	Att: R. A. Marsh
	    D. M. Ryan
	WL/POOS-2
	1950 Fifth St.
	Wright-Paterson AFB, OH 45433-7251
		5	Eagle-Picher Industries, Inc.
			Electronics Div. Couples Dept.
			Attn: R. Spencer
			    F. Smith
			    J. DeGruson
			    R. Hudson
			    J. Wells
			P.O. Box 47
			Joplin, MO 64802

4	Argonne National Laboratory
	Chemical Technology Div.
	Attn: D. Vissers
	    L. Redey
	    J. Smaga
	    T. Kaun
	9700 South Cass Ave.
	Argonne, IL 604339
		2	General Dynamics Pomona Div.
			Attn: Kathy Wong
			    Jaime Perez
			Mail Zone 4-66
			P. O. Box 2507
			Pomona, CA 91769-2507

2	Army Materials and Mechanism Research Center Attn: J. W. McCauley P. Wong Watertown, MA 02172	1	Hughes Aircraft Co. Attn: L. A. Schaum, Jr. Building 803 Mail Station E P. O. Box 11337 Tuscon Az. 85721
2	Army Research Lab Attn: F. Krieger A. Goldberg 2800 Powder Mill Road Adelphi, MD. 20783	1	Martin-Marietta Specialty Components Div. Attn: W. McCracken P.O. Box 2908 Largo, FL 34649
1	A. A. Benderly, Consultant 9915 Logan Dr. Potomac, Maryland 20854	1	Naval Ordnance Station Attn: K. Englander Code 5123C Indian Head, MD 20640

3	Boeing Aerospace
	Attn: C. Johnson
	    J. Kavandi
	    Sid Gross
	P. O. Box 3999
	Seattle, WA 98124
		2	Naval Surface Warfare Center
			Attn: B. Larrick
			    C. E. Mueller
			Silver Springs, MD. 20910

1		Naval Surface Warfare Center Attn: C. Winchester Code R33 10901 New Hampshire Ave. Silver Spring, MD 20903-5000
1		Naval Underwater Systems Center Attn: R. S. Lazar Code 36301 Newport, RI 02840
3		Naval Weapons Center Attn: M. H. Miles R. Nolan (Code 3626) D. Rosenlof (Code 3626) China Lake, CA 93555
1		Parker Hannifin Attn: Arvind Ahluwalia, MS K141 14300 Alton Parkway Irvine, CA 92718-1814
2		SAFT America Attn: K. K. Press J. Embrey 107 Beaver Court Cockeysville, MD 21030
1		Technochem CO. Attn: Shyam Argade 203A Creekridge Rd. Greensboro, NC 27406
2		Westinghouse Electric Corp. Att: Nick Shuster Nick Pappadakis 18901 Euclid Ave. Cleveland, OH 44117

4		Defense Research Agency Materials Dept. Attn: J. Knight A. G. Ritchie Building R178 Farnborough Hants GU14 6TD ENGLAND
1		Leclanche, S.A. Attn: P. Reutschi 48, Avenue de Grandson CH-1401 Yverdon-Les-Bain SWITZERLAND

1	MS0614	A. H. Andazola, 2222
1	0614	J. A. Gilbert, 2222
1	0614	K. R. Grothaus, 2223
5	0614	R. A. Guidotti, 2223
1	0614	F. P. Lasky, 2222
1	0614	D. E. Mitchell, 2222
1	0614	L. M. Moya, 2222
1	0614	F. W. Reinhardt, 2223
1	0614	G. L. Scharrer, 2222
2	0161	M. Moss, 11500
1	9018	Central Technical Files, 8523-2
1	0899	Technical Library, 13414
1	0619	Print Media, 12615
2	0100	Document Processing, 7613-2 For DOE/OSTI

21